Supporting Information

Dasgupta et al. 10.1073/pnas.0911028106

SI Materials and Methods

Fly Stocks and Husbandry. *Drosophila* stocks were raised on standard corn meal agar and maintained at 25 °C unless otherwise mentioned. The DCERK P elements, Δ 2–3 transposase and *norp A* null mutants were obtained from the Bloomington Stock Center; *DTS5* flies were from Dr. Eric Baerahcke, University of Massachusetts Medical School; PLCδPH GFP flies were from Dr. Andy Zelhof, Indiana University. DCERK cDNA (EST AT18965) was cloned into the pUAST vector as a NotI-XhoI fragment. This construct was injected into w^{1118} embryos using standard techniques to generate transgenic flies. UAS DCERK transgenic flies were driven by actinGAL4 driver to rescue $dcerk^{1}$ phenotypes. PLCδPHGFP; Gmr-Gal4cn.bw/cn.bw; + flies were generated to check for PLCGFP expression and staining with GFP antibody. For PIP3 expression, Gmr-Gal4cn.bw/cn.bw; GRP1PHGFP/+ flies were generated and photoreceptors sections from these flies were stained with GFP antibody.

Genetic Screen and Isolation of *dcerk* Mutants. DCERK P-element (w^{1118}; P{GT1}CG16708BG01100, Bloomington Stock Center, stock# 12454) females were crossed to Δ 2–3 transposase males. Single dysgenic males were crossed to balancer females, and potential jump-out males and females were collected and homozygous stocks generated. One fly head from each viable line was processed for western analysis and probed with a monoclonal antibody to DCERK to check for loss or reduction in DCERK protein. Five hypomorphic mutants including $dcerk^{1}$ were isolated from the screen.

Immunohistochemistry

Antibodies. Mouse monoclonal antibodies to CERK was raised against bacterially expressed and gel purified DCERK. A 1.2-kb N-terminal fragment and 1.2-kb C-terminal fragment of DCERK were cloned as SalI-HindIII fragments into pMalc2x. These fragments were expressed and gel purified by electroelution. The purified N- and C- fragments were injected into mice and several monoclonal antibodies were generated.

Monoclonal antibody 3H7 was used in this study. Antibodies to Gα, INAD, NORPA, Arrestin1, Arrestin2, RDGC, TRP, Rhodopsin 1 were kind gifts from Dr. Charles Zuker, University of California, San Diego; antibody against NINAC was from Dr. Craig Montell, Johns Hopkins University, antibody to Lava Lamp was from Dr. John Sisson, University of Austin, antibody against TRPL was from Dr. Hong-Sheng Li, University of Massachusetts Medical School, Worcester; antibodies to Rab5 and Calnexin were from Abcam (Cambridge, MA) and antibody to PIP_2 was from Assay Designs (Ann Arbor, MI). The Tubulin monoclonal antibody (E7) and Rhodopsin monoclonal antibody (4C5) were obtained from Developmental Studies Hybridoma Bank under the auspices of the National Institute of Child Health and Human Development and maintained by University of Iowa, Department of Biological Sciences. Secondary antibodies for immunostaining were obtained from Invitrogen. For the biotinylation experiments, biotinylated affinity purified anti-mouse IgG, fluorescein-conjugated streptavidin and the blocking kit were obtained from Vector Labs (Burlingame, CA).

Antibody Staining of Imaginal Discs and *Drosophila* S2 Cells. Fixation and staining of third instar larval imaginal discs and S2 cells were carried out as described earlier (12). For imaginal discs and S2 cells, DCERK antibody was used at (1:50), Scramblase (1:250), Cadherin (1:25) Rab5 (1:400), Lava Lamp (1:1000), Calnexin (1:400), and secondary antibodies were used at 1:1500 dilution. Biotinylated affinity purified anti-mouse IgG was used at 1:500, and fluorescein-conjugated streptavidin was at 1:100 dilution.

Immunofluorescence of Photoreceptor Cells. Thin eye sections (0.5 μm) were blocked in PBT (phosphate-buffered saline [PBS] + 0.1% Tween-20) + 3% bovine serum albumin (BSA) and 2% normal goat serum for 1 h, stained with primary antibody for 2 h, washed with PBT, and stained with secondary antibody for 1 h, washed, and mounted. The sections were stained with mouse anti-DCERK (1:5), rabbit anti-Rh1 (1:100), rabbit anti-NORPA (1:50), rabbit anti-INAD (1:50), rabbit anti-TRP (1: 20, preadsorbed on w^{1118} head extract for 2 h), mouse anti-PIP_2 (1:200), Cadherin (1:20), GFP antibody (1:300), and secondary antibodies (1:1000). Stained sections were visualized using Zeiss Axioplan imaging system using Hamamatsu-ORCA-ER camera and Axiovision 4.5 software. Quantum dot 565 goat anti-mouse Fab_2 was used at 1:500 dilution, and the sections were viewed using Q dot filter sets on a spinning disc microscope (Solamere Technology Group modified Yokogawa CSU10 Spinning Disk Confocal).

Morphometric analysis was performed on confocal images of photoreceptors using Metamorph program 7.1 (Universal Imaging, Downingtown, PA). Pixel to micron ratio was assigned and the program measured area of PIP_2 stained structures. In each condition, several images were taken to cover the whole eye, and then the area of PIP_2 stained structures was averaged for the whole eye. The results denote a final average of three whole eyes from three independent experiments.

Purification and Enzyme Assay for CERK Activity. DCERK protein was isolated from stable *Drosophila* S2 cell line expressing His-V5 tagged DCERK. Cell pellet from 80 ml of induced S2 cells expressing DCERK was resuspended in lysis buffer (10 mM Mops pH 7.2, 150 mM KCl, 1 mM EDTA, 5 mM DTT, Protease Inhibitor Mixture (Sigma) and dounced in a glass homegenizer. The cell lysate was centrifuged at 100,000 *g* for 1 h. The pellet was re-suspended in 10 mM Mops pH 7.2, 150 mM KCl, 10% glycerol, 0.5% Triton X-100, Protease Inhibitor Mixture, and incubated at 4 °C for 1 h with gentle swirling. The re-suspended membrane fraction was centrifuged at 30,000 *g* for 30 min and the supernatant passed through His-Spin Trap column (GE Healthcare). DCERK protein was eluted with 300 mM imidazole buffer containing 0.5% Triton X-100 and used for assays. The assay for CERK activity was carried out according to the procedure described before with minor modifications (15). Ceramide (0.25 mM) with a sphingoid backbone of d_{18} and fatty acyl chain of C_{16} and sphingosine were dried under nitrogen and resuspended in solution containing 5 mM cardiolipin, 20 mM Mops, 1 mM diethylenetriaminepentaacetic acid pH6.6, 7.5% β-octyl glucoside, 50 mM NaCl, 1 mM DTT, and 10 mM $CaCl_2$. The mixture was vortexed and sonicated in a bath sonicator for 15 min, after which ATP was added. This mixture was then added to a 96-well assay plate (Microlite1+, Thermo Scientific); the final assay wells contained 250 μm ceramide, 12.5 μm ATP, and 5 μg of purified DCERK protein. Reactions were performed in duplicate and incubated for 1 h at 28°C. After incubation, 50 μl of Kinase glo (Kinase-Glo, Promega Corporation) was added to each reaction, mixed well and read on a Counter using Wallac 1420 software (Victor^3 1420 Multilabel, Perkin-Elmer Life

Sciences). DCERK activity was measured as a decrease in ATP concentration using Kinase-Glo luminescent signal.

Molecular Techniques

RT-PCR Analysis. RNA was isolated from whole flies using TRIzol reagent (Invitrogen). A 200-ng quantity of DNaseI treated RNA sample was amplified by SuperScript One-Step RT-PCR System using *DCERK* 5′ATGACGCAGACCAAGCAGCCAGCA 3′; 5′ AAAACAATGACGGG GAGACCC 3′. These two primers, RT-PCR the full length ORF of CG16708, a length of 2186 nucleotides. The genomic fragment would be 2674 nucleotides due to inclusion of two introns. The primers for *Actin* 5′ATGTGTGACGAAGAAGTTGCTGCT 3′; 5′ TTAGAAGCACTTGCGGTGCA CAATG 3′ include the ORF of actin 5C, a length of 1.13kB.

Real-Time PCR Analysis. RNA was isolated from fly retina using TRIzol reagent. Approximately 1 μg RNA was reverse transcribed using SuperScript II reverse transcriptase with Oligo(dT)$_{12–18}$ (Invitrogen). Real-time PCR was performed using SYBR Green PCR mastermix and the ABI PRISM 7000 Sequence Detection System (Applied Biosystems). The primers used were as follows: *NORPA* 5′GGGCAGGGATGGCGATGTCAT3′ and 5′ TTGGCT, GTTGCCGCATCTGG3′; *RP49* 5′AAGCTGTCGCACAAATGGCG 3′, and 5′GCACGTTGTGCACCAGGAAC3′. The Ct values for NORPA were normalized using the values of RP49 to obtain the DCt. The DCt values for W^{1118} and $dcerk^1$ were divided with the DCt value of W^{1118} to obtain DDCt.

ERG Recordings. ERG recordings were performed as described before (1). Electrical signals were amplified using a DAM50 amplifier (World Precision Instruments), recorded using Powerlab 4/30, viewed and analyzed using Chart 5 software (AD Instruments, Colorado Springs, CO). Stimulating light was generated with a halogen lamp controlled by a Model T132 Uniblitz shutter. All light pulses were 1 s in duration and at maximum intensity using 580-nm band-pass filters. All recordings were performed on adult flies that were reared in the dark.

Estimation of PIP_2 in Fly Head Extracts. All lipids were obtained for Avanti Polar Lipids Inc (Alabaster, AL). Flies were raised in the dark and heads were cut from 1-day old frozen flies (200 flies/sample). Lipids were extracted by adapting a protocol described earlier (2). Frozen fly heads were homogenized in 500 μl methanol:chloroform (2:1) using a Teflon homogenizer in a 1.5-ml microcentrifuge tube. The homogenate was transferred to a glass tube and 1.5 ml of methanol:chloroform (2:1) was added, followed by 500 μl of water and vortexed. The homogenate was sonicated in a water bath type sonicator for 20 min and incubated overnight at 37 °C. To the extract 1 ml of water and 500 μl chloroform were added, vortexed, and centrifuged at 1000 rpm for 10 min at room temperature. The organic phase was collected and dried under nitrogen. Extracts were redissolved in 2 ml synthetic upper (methanol:water:chloroform, 94:96:6) and applied to pretreated SepPak C18 column for solid phase extraction (Waters). The column was washed with 4 ml of water and lipids extracted in 4 ml of methanol followed by 4 ml of methanol:chloroform. The samples were dried under nitrogen and redissolved in requisite amount of chloroform:methanol (1:1). A portion of each sample was used to estimate total lipid by charring with sulfuric acid (3). Lipids extracted from w^{1118}, $dcerk^1$, and rescue ($dcerk^1$ expressing DCERK) flies were run on pretreated thin-layer chromatography (TLC) plates (Partisil LK6D, Silica gel 60A, 5 × 20 cm, Whatman, England) along with PIP_2 standard using a two-solvent one-dimensional TLC (4). The TLC plate was sprayed with 0.05% primuline to visualize the standard, and the silica gel region corresponding to standard PIP_2 was scraped out from sample lanes. Lipids were extracted from silica with chloroform:methanol (1:1) twice and the supernatant dried under nitrogen.

Estimation of PIP_2 by ELISA. Polystyrene-coated, 96-well, flat-bottomed ELISA plates (BD Biosciences) were coated with 20 μl ethanol followed by standard PIP_2, dissolved in chloroform:methanol:water (1:2:0.8) in a range of 1–100 pmol. The plate was dried overnight at room temperature. The experimental samples were also dissolved similarly and coated on the same plate. All samples were blocked with 3% BSA in PBS for 2 h followed by washes with 0.1% Tween-PBS and incubated with PIP_2 antibody (1:1,000) for 2 h and horseradish peroxidase (HRP)–conjugated secondary antibody (1:5,000) for 1 h. The plate was washed and developed with 1-Step Ultra TMB-ELISA substrate (Pierce), and the reaction was allowed to proceed until blue color developed. The reaction was stopped using 2 M sulfuric acid and was read at 450 nm on a microplate reader (Synergy HT Multi Detection, Bio-Tek Instruments). Sample data were plotted after generating a standard curve for PIP_2.

Estimation of Sphingolipids by Mass Spectrometry. Liquid chromatography was performed on an ACQUITY UPLC BEH Shield RP18 column (100 mm × 2.1 mm) maintained at 60 °C. The mobile phase was composed of 5 mM ammonium formate in water containing 0.2% formic acid (solvent A) and 5 mM ammonium formate in methanol containing 0.2% formic acid (solvent B) with a flow rate of 0.3 ml/min. Elution conditions involved an isocratic elution using 20% solvent A for 5 min followed by a linear gradient from 80% to 98% solvent B for 1 min and then again isocratic elution with 98% solvent B for 6 min. For mass-spectrometric measurements (Quattro Premier XE, Waters), quantification was performed using Selected Reaction Monitoring (SRM) of ceramide: 18:0 (precursor 510.5, product 208.3); 20:0 (538.5); 22:0 (566.5), and 24:0 (594.6). The SRM for ceramide 1-phosphate was 18:0 (precursor 590.5, product 208.3); 20:0 (618.5); 22:0 (646.5), and 24:0 (674.5). The following parameters were used: a capillary voltage of 2.0 kV, source temperature 120 °C and desolvation temperature of 450 °C. Nitrogen was added as desolvation and cone gas with flow rates of 1,000 and 50 L/h respectively. Argon was used as the collision gas at a pressure of 4.3×10^{-3} mbar.

Fluorescence Polarization Measurements. The isolation of plasma membrane and fluorescence polarization measurements were performed as described before (22). Plasma membrane was isolated by density gradient centrifugation. Flies were washed thoroughly in PBS containing 0.5% Triton X-100 to remove the residual food material sticking to the flies and were homogenized in homogenization buffer [100 mM Tris·HCl (pH 7.4)/150 mM sodium chloride/0.2 mM EGTA with protease inhibitor mixture]. The homogenate was centrifuged at 1,000 × g for 10 min to remove cell debris. The resulting postnuclear supernatant was mixed 1:2 with Opti-Prep, resulting in 40% solution. Optiprep solutions (30% and 5%) were overlaid on the top. The tubes were centrifuged for 3 h at 100,000 g. Plasma membrane appeared as a white dense band at 30–5% interface. The membrane was collected and used immediately for fluorescence polarization studies. TMA-DPH was added (500 pmol/mg of protein) to membranes and suspended in 1 ml of 50 mM potassium phosphate buffer (pH 7.4), and the mixture was incubated at 25 °C for 30 min with gentle shaking. Fluorescence polarization was measured in FluoroMax-2 spectrofluorimeter (ISA) with 360-nm excitation and 430-nm emission wavelengths. Fluorescence intensities in both parallel and perpendicular directions to the incident light were measured, and fluorescence

polarization was calculated. Membrane fluidity was expressed as the inverse function of polarization.

Preparation of Supported Lipid Bilayers. All unlabeled lipids were purchased from Avanti Polar Lipids (Alabaster) and used without further purification. Briefly, unlabeled lipids and fluorescent PIP_2 (BodTMRPIP$_2$, Echelon Bioscience, Salt Lake City, UT) were mixed in organic solutions in different proportions. For bilayers showing no phase separation, the lipid composition was either 100% molar dioleoylphosphatidylcholine (DOPC), 97% DOPC + 3% brain PIP2 (BrPIP$_2$), 92% DOPC + 3% BrPIP$_2$ + 5% cholesterol, or 92% DOPC + 3% BrPIP$_2$ + 5% ceramide. Ceramides were either synthetic C6 or brain extract species. For bilayers showing phase separation, we used two different lipid mixtures. To obtain L_o/L_d phase separation, we mixed 37.5% molar DOPC + 37.5% C18:0 sphingomyelin (SM) + 25% cholesterol. To obtain ceramide/L_d phase separation, we mixed 37.5% DOPC + 21.5% SM + 16% C18:0 ceramide + 25% cholesterol. Cholesteryl-4,4-difluoro-5,7-dimethyl-4-bora-3a,4a-diaza-*s*-indacene-3-dodecanoate (BodChol, Invitrogen, Eugene, OR) was added in 0.01% molar proportion to visualize the L_d phase. The concentration of BodTMRPIP$_2$ was 0.005 mol% in all cases. After solvent evaporation, the lipid film thus obtained was slowly rehydrated using PBS buffer without Ca^{2+}/Mg^{2+} at 10 mg/ml lipid concentration and resuspended through vigorous vortexing. After sonicating the suspension at 65 °C, a small aliquot was diluted to 0.5 mg/ml in SLB buffer (10 mM Hepes, 150 mM NaCl, 3 mM NaN_3, pH 7.4) and deposited on a ≈10-μm thick, freshly cleaved mica, glued to a glass coverslip. A 2-mM quantity of Ca^{2+} was added to promote vesicle adhesion and fusion onto the mica surface. After 15 min incubation at 65 °C, the sample was rinsed at high temperature at least 10 times with 2 mM Ca^{2+} SLB buffer and then allowed to cool to 25 °C. Samples showing phase separation were washed first with 15 mM EDTA SLB buffer and finally with 0.1 mM EDTA SLB buffer to remove the Ca^{2+} ions needed for vesicle fusion.

Samples treated with GAP43 were prepared by a procedure adapted from previously published protocols (5). Liposomes were prepared as described above for the phase separation mixtures. After brief sonication, liposomes in SLB buffer (1 mg/ml) were incubated for 1 h at 40 °C with 1 mM DTT, 15 μM palmitoyl CoA, and 3 μM GAP-43 derived peptide (GAP-43P, synthesized by Bachem, Torrance, CA). Subsequently, the liposomes were briefly sonicated again and transferred to the mica surface, as described above for the phase separating bilayers (i.e., in presence of EDTA).

Fluorescence Imaging and Image Correlation Spectroscopy. Fluorescence imaging was performed at room temperature (≈25 °C) on a LSM 510 Meta (Zeiss, Jena, Germany). The excitation light of a Argon laser at 488 nm (or He-Ne 543 nm) was reflected by a HFT 488 (or HFT 700/543) dichroic mirror and focused onto the sample by a Zeiss C-Apochromat 40x, NA = 1.2 UV-VIS-IR water immersion objective. Fluorescence signal was then recollected by the same objective and, after passing through a 525/50 bandpass (or 560-long pass) filter, measured by a photomultiplier (PMT). The confocal geometry was ensured by a 70 (80) μm pinhole in front of the PMT.

Image correlation spectroscopy (ICS) was performed as described before (6). For each sample, 16–24 23 × 23-μm^2 images from two different preparations were acquired in the red channel. The width of a pixel was ≈40 nm. A self-written Matlab program (MathWorks, Natick, MA) performed background and white noise correction, and the calculation of the autocorrelation matrix, which was fitted using a 2-d Gaussian. The cluster density CD was calculated from the fit parameters. Provided that the amount of BodTMRPIP$_2$ molecules is constant in the different samples and that the cluster dimensions are never larger than the optical resolution, the degree of clustering is defined as the inverse of CD (at high cluster density, the clusters are smaller with fewer fluorophores; at low cluster density, there are many fluorophores per cluster).

Measurement of BodTMRPIP$_2$ partition into Lo domains was performed acquiring fluorescence images in both red and green channels. A self-written Matlab program performed the following: (*i*) background correction, (*ii*) precise spatial alignment of the two channels via a cross-correlation algorithm; (*iii*) phase assignment using the signal in the green channel; and (*iv*) calculation of the partition defined as $\langle I_{Lo}^{BodTMRPIP2}\rangle_{LoPixles}/\langle I_{Lo}^{BodTMRPIP2}\rangle_{LdPixles}$, i.e., the ratio between the fluorescence signal from BodTMRPIP$_2$ in the L_o phase (averaged over all of the pixels in the L_o phase) and the fluorescence signal from BodTMRPIP$_2$ in the L_d phase (averaged over all of the pixels in the L_d phase). For each sample, we acquired 16–24 images from two different bilayer preparations. Image dimensions varied between ≈15 × 15 and 23 × 23 μm^2. Statistical significance of the variations between samples was assessed using the "ttest2" routine from Matlab (1% or 10% significance level).

1. Gavin BA, Arruda SE, Dolph PJ (2007) The role of carcinine in signaling at the Drosophila photoreceptor synapse. *PLoS Genet* 3:e206.
2. Merrill AH, Jr., Sullards MC, Allegood JC, Kelly S, Wang E (2005) Sphingolipidomics: High-throughput, structure-specific, and quantitative analysis of sphingolipids by liquid chromatography tandem mass spectrometry. *Methods* 36:207–224.
3. Marsh JB, Weinstein DB (1966) Simple charring method for determination of lipids. *J Lipid Res* 7:574–576.
4. Medh JD, Weigel PH (1989) Separation of phosphatidylinositols and other phospholipids by two-step one-dimensional thin-layer chromatography. *J Lipid Res* 30:761–764.
5. Quesnel S, Silvius JR (1994) Cysteine-containing peptide sequences exhibit facile uncatalyzed transacylation and acyl-CoA-dependent acylation at the lipid bilayer interface. *Biochemistry* 33:13340–13348.
6. Nohe A, Petersen NO (2007) Image correlation spectroscopy. *Sci STKE* 417:17.

Sequence Alignment of CERKs and human CERKL

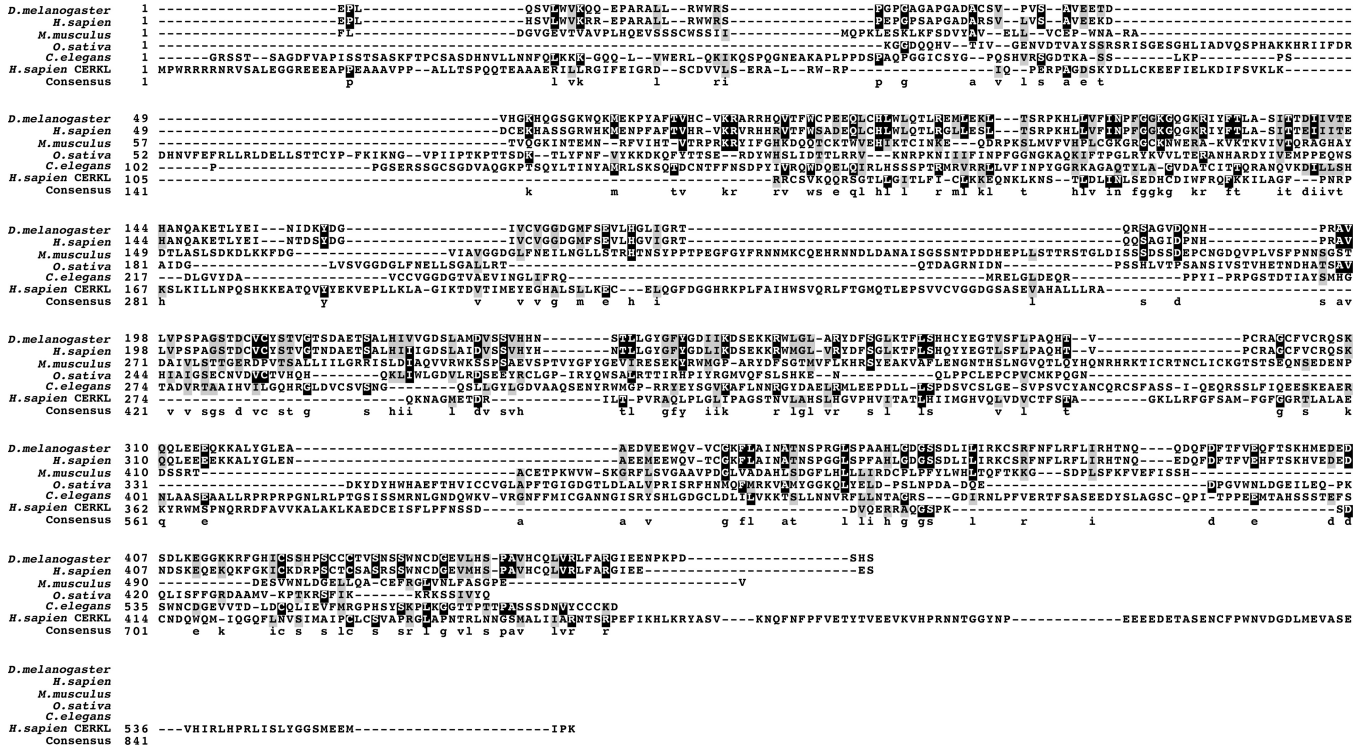

Fig. S1. Comparison of the amino acid sequences of CERK homologs from *Drosophila*, human, mouse, *C.elegans,* and rice and human CERKL.

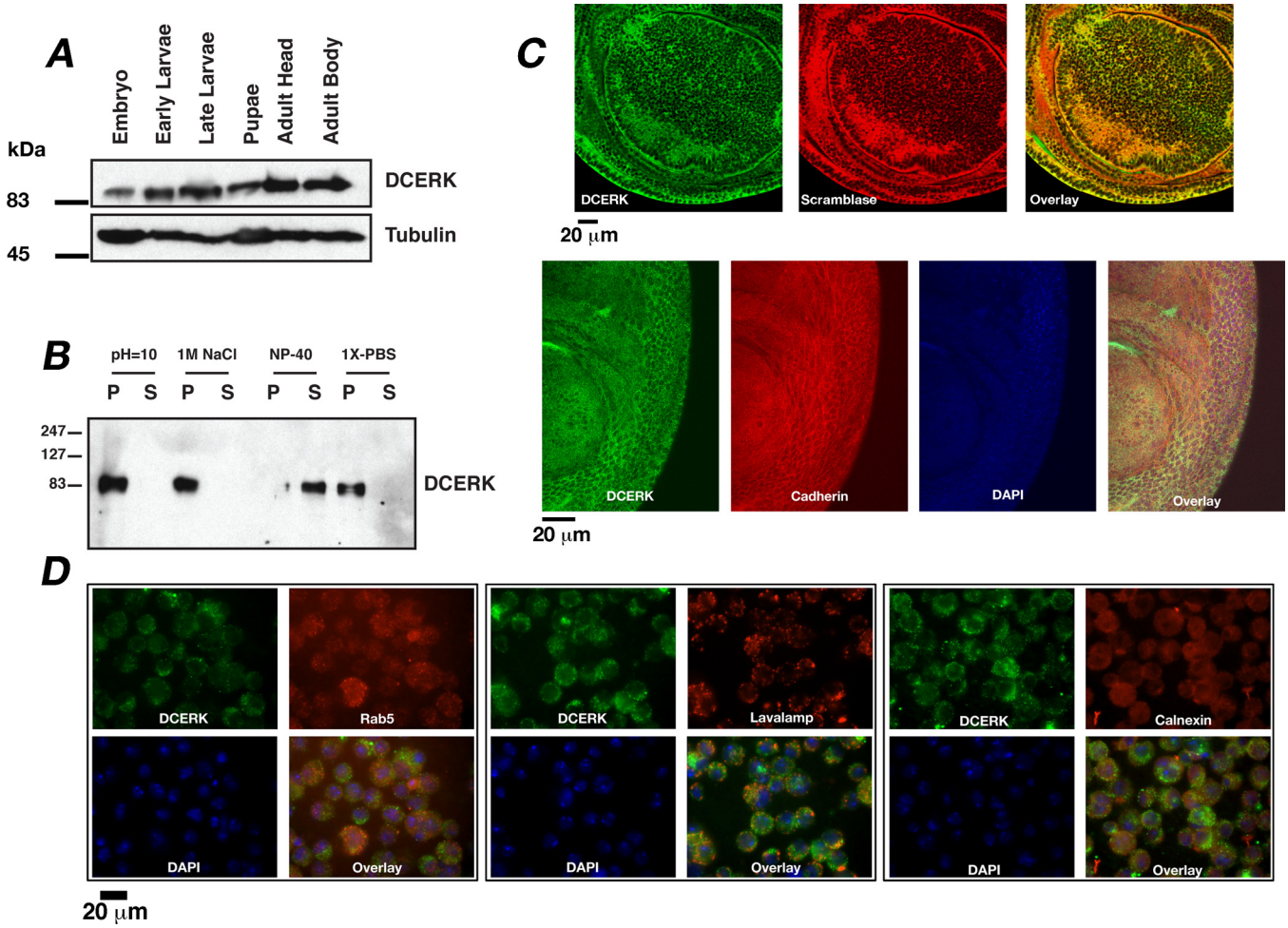

Fig. S2. Characterization of *Drosophila melanogaster* CERK (DCERK). (*A*) Protein extracts prepared at different stages of *Drosophila* development are separated by sodium dodecyl sulfate/polyacrylamide gel electrophoresis (SDS/PAGE), blotted and probed with a monoclonal antibody (3H7) to DCERK. The blot shows that DCERK is ubiquitously expressed. The blot is also probed for tubulin as a loading control. (*B*) Fractionation of head extracts shows that DCERK is an integral membrane protein. DCERK could be dissociated from the membrane by treatment with the detergent Nonidet P-40 but not by alkaline pH or high salt concentration. (*C*) *Upper panel* shows wing imaginal discs co-stained with an antibody to scramblase, a protein previously demonstrated to localize to the plasma membrane. (Scale bar, 20 μm.) *Lower panel* shows immunostaining with an antibody to cadherin. (Scale bar, 20 μm.) (*D*) DCERK does not co-localize with endosome, Golgi, or ER markers. Schneider cells were stained with a monoclonal antibody to DCERK and rabbit polyclonal antibodies to Rab5 (endosomal marker), Lava Lamp (Golgi marker), Calnexin (ER marker), and DAPI to stain the nucleus. Overlay images show there is no significant overlap between DCERK and these organelle markers.

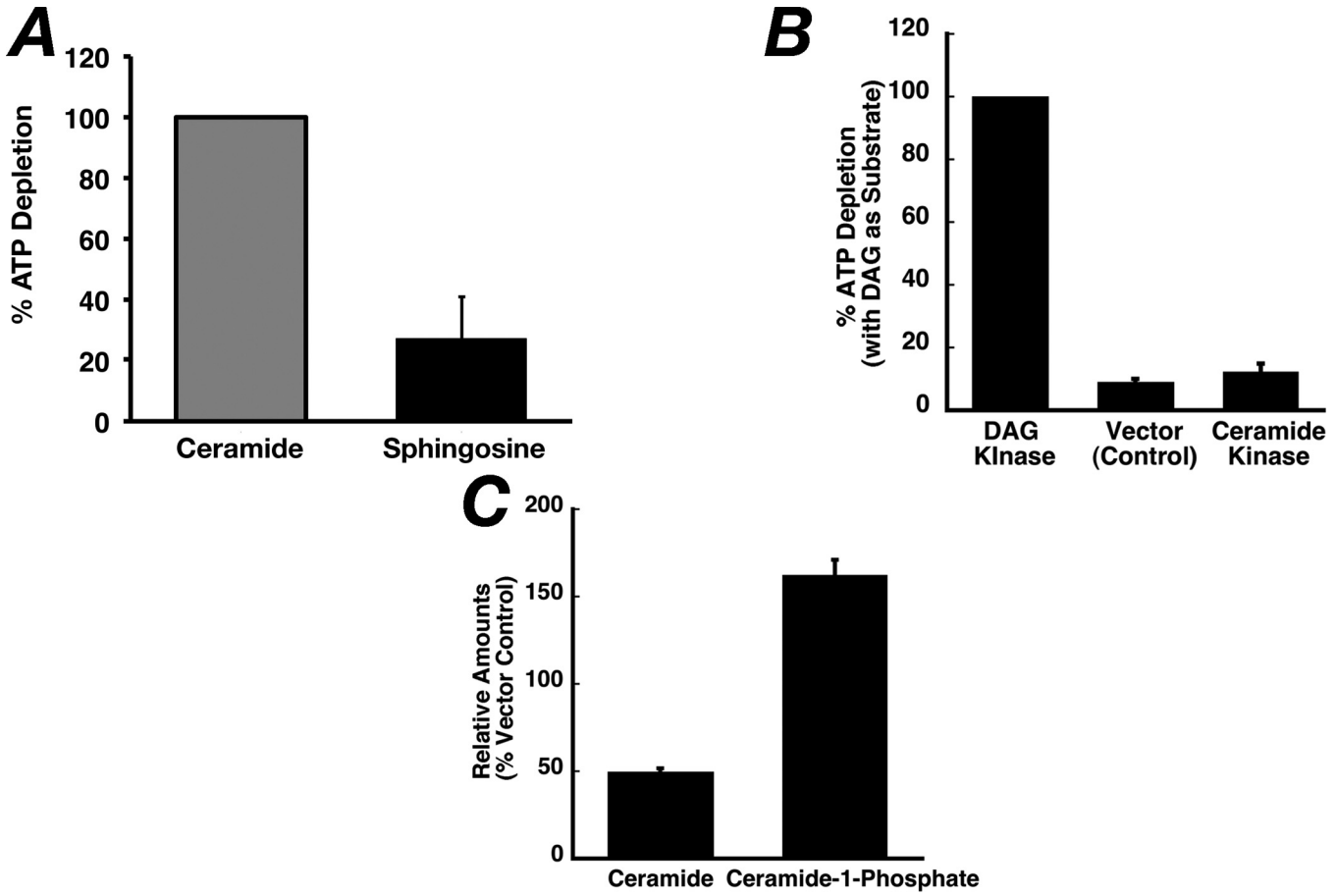

Fig. S3. DCERK is a bona fide ceramide kinase. (*A*) The ability of DCERK to deplete ATP in the presence of ceramide or sphingosine is measured by a chemiluminescence assay. Membrane fractions from Schneider cells stably expressing either vector alone or DCERK were used in the assay. DCERK phosphorylates ceramide significantly ($n = 3$). Error bar denotes standard deviation. (*B*) DCERK does not use DAG as a substrate. The ability of DCERK to deplete ATP is measured by the chemiluminescence assay using DAG as substrate. Purified DAG kinase was used a positive control in this assay. (*C*) DCERK expression results in decreased ceramide and increased ceramide-1-phosphate levels. Lipid extracts were prepared from Schneider cells stably expressing either vector alone or DCERK and subjected to mass spectrometry. Cells expressing DCERK show 50% reduction in ceramide and ≈60% increase in ceramide-1-phosphate when compared with cells expressing vector alone.

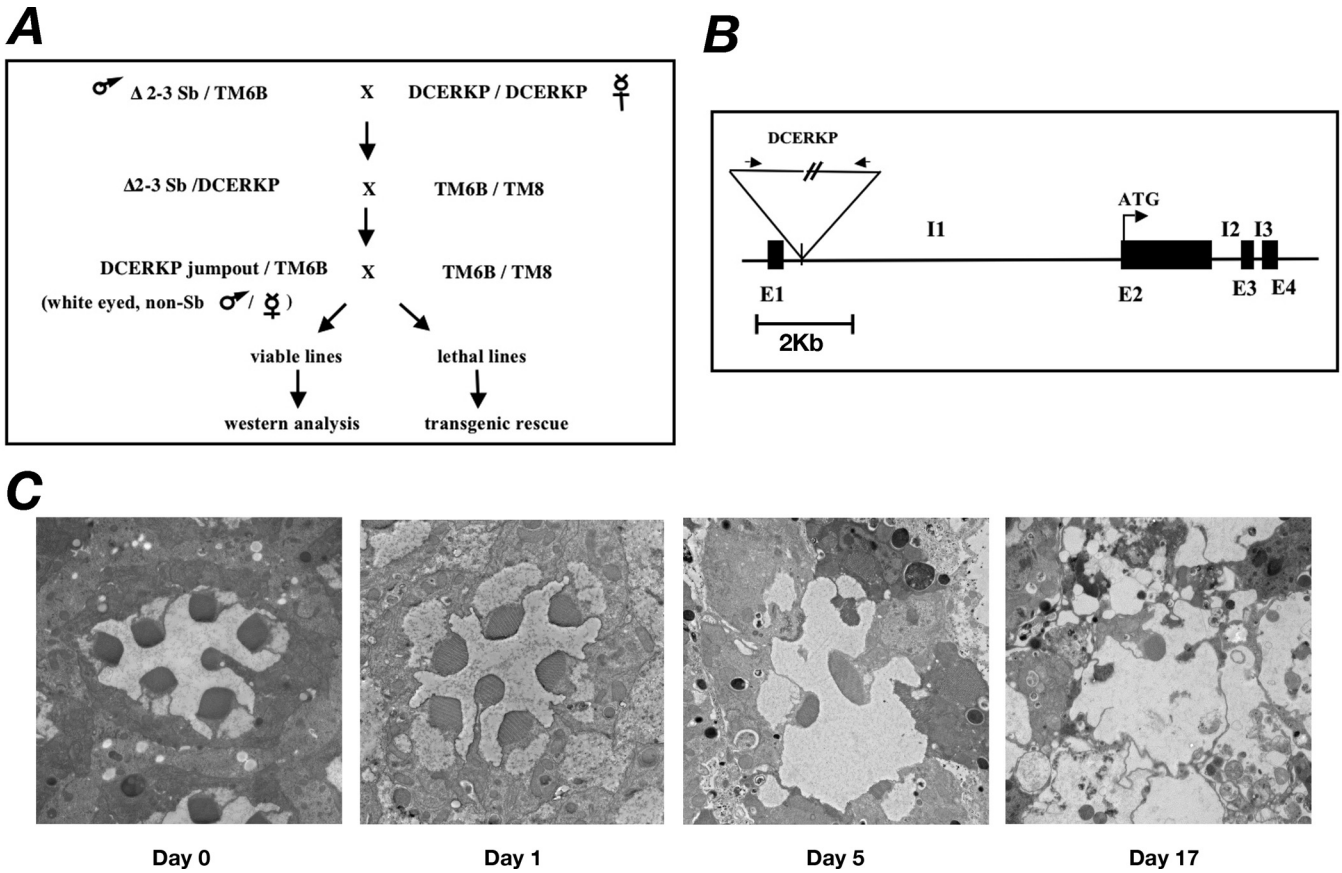

Fig. S4. Genetic scheme used to isolate *dcerk* mutants. (*A*) P element (w^{1118}; P{GT1}CG16708BG01100, Bloomington Stock Center, stock# 12454) was mobilized and excision lines were established. Western analysis using 3H7 antibody to DCERK was carried out on one fly head sample from each viable line while lethal lines were analyzed by rescue experiments with a transgenic fly expressing DCERK. (*B*) PCR and sequence analysis of genomic DNA revealed that ≈6 kb (shown by arrows) of the original 11.2kb P element was left behind in $dcerk^1$. (*C*) Light induced progressive degeneration in $dcerk^1$. Transmission electron micrographs show photoreceptors of newly eclosed, 1-, 5-, and 17-day-old $dcerk^1$ mutants. Rhabdomeres can be seen in newly eclosed and 1-day-old photoreceptors, whereas those of 5- and 17-day-old flies show hardly any rhabdomeres and extensive vacuolation.

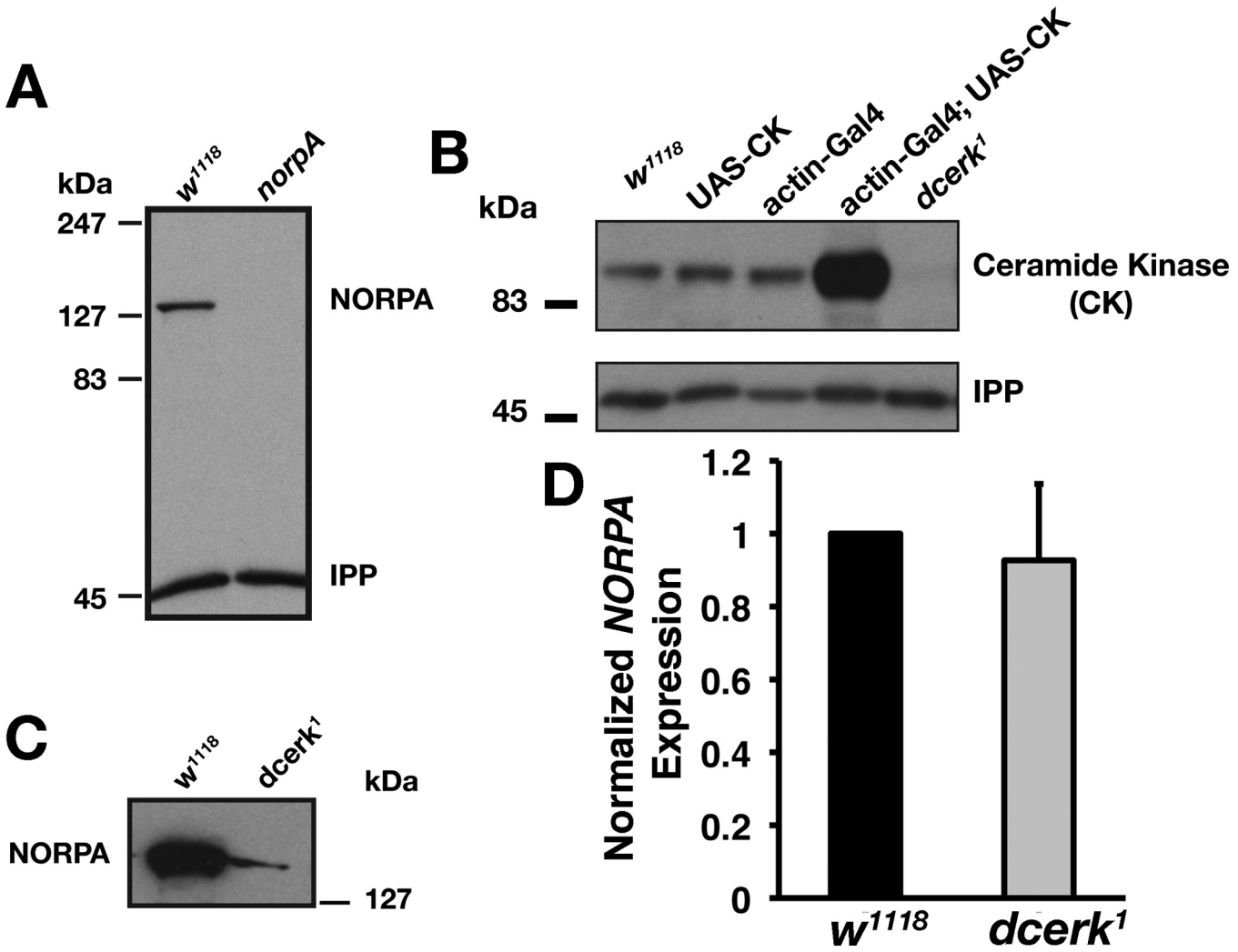

Fig. S5. NORPA level is down regulated in *dcerk*^{1}. (*A*) Western analysis of *w*^{1118} and *norpA* null mutant head extracts probed for NORPA showing specificity of the NORPA antibody used in the study. The blot is probed with an antibody to IPP as loading control. (*B*) The level of ceramide kinase over-expression when UAS-CERK transgenic flies are driven using the actin GAL4 driver. Western blot of head extracts from 1-day-old dark-raised *w*^{1118}, CERK transgenic alone (UAS-CK), driver alone (actin GAL4), actin GAL4 driven CERK transgenic (actin Gal4.UASCK) and *dcerk*^{1} flies. CERK is overexpressed significantly in the actin Gal4 driven flies. (*C*) A small amount of NORPA protein can be detected in 1-day-old dark-raised flies when the Western blot is significantly overexposed. (*D*) DCERK modulates NORPA posttranscriptionally. Real time PCR analysis of RNA isolated from *w*^{1118} and *dcerk*^{1} shows that DCERK primarily modulates *NorpA* posttranscriptionally. $n = 5$. Error bars denote standard deviation.

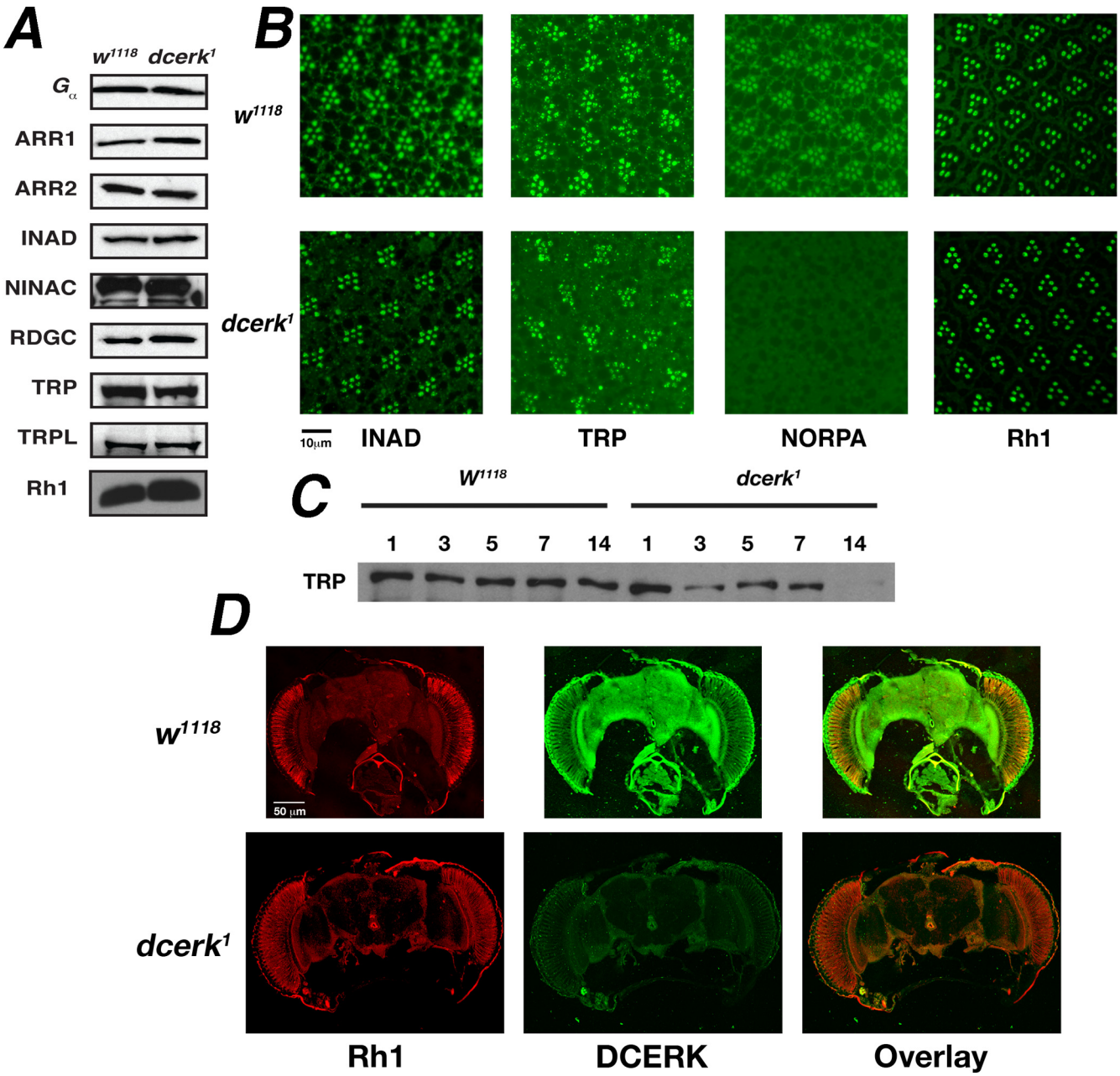

Fig. S6. Levels and localization of other phototransduction components are not significantly affected in *dcerk*^{1} mutants. (*A*) Western analyses of various phototransduction components show that their levels are not changed in 1-day-old *dcerk*^{1} compared with *w*^{1118} extracts. (*B*) Thin sections of dark-grown *w*^{1118} and *dcerk*^{1} photoreceptors are stained with antibodies against different phototransduction components. Immunostaining reveals that localization of INAD, TRP, and rhodopsin 1 (Rh1) proteins remain unaffected in *dcerk*^{1}. (*C*) Western analysis showing TRP protein is lost by day 14 in *dcerk*^{1} compared with *w*^{1118}. (*D*) Immunostaining of eyes with antibodies to DCERK and Rh1. Cryosections (10 μm) were co-stained for Rh1 (red, as a control marker for rhabdomere in R1-R6) and DCERK (green). *Upper panel* shows cryosection of *w*^{1118} at $\times$10 magnification; *lower panel* shows *dcerk*^{1}. These sections provide a view of the photoreceptors, underlying lamina, and the brain. In the control sections, CERK is present in the rhabdomeres and other membranous compartments of photoreceptors, overlying cone and lens cells, underlying lamina, and brain, whereas Rh1 shows specific rhabdomere staining of R1-R6 cells. The DCERK staining in the mutant is at the background level.

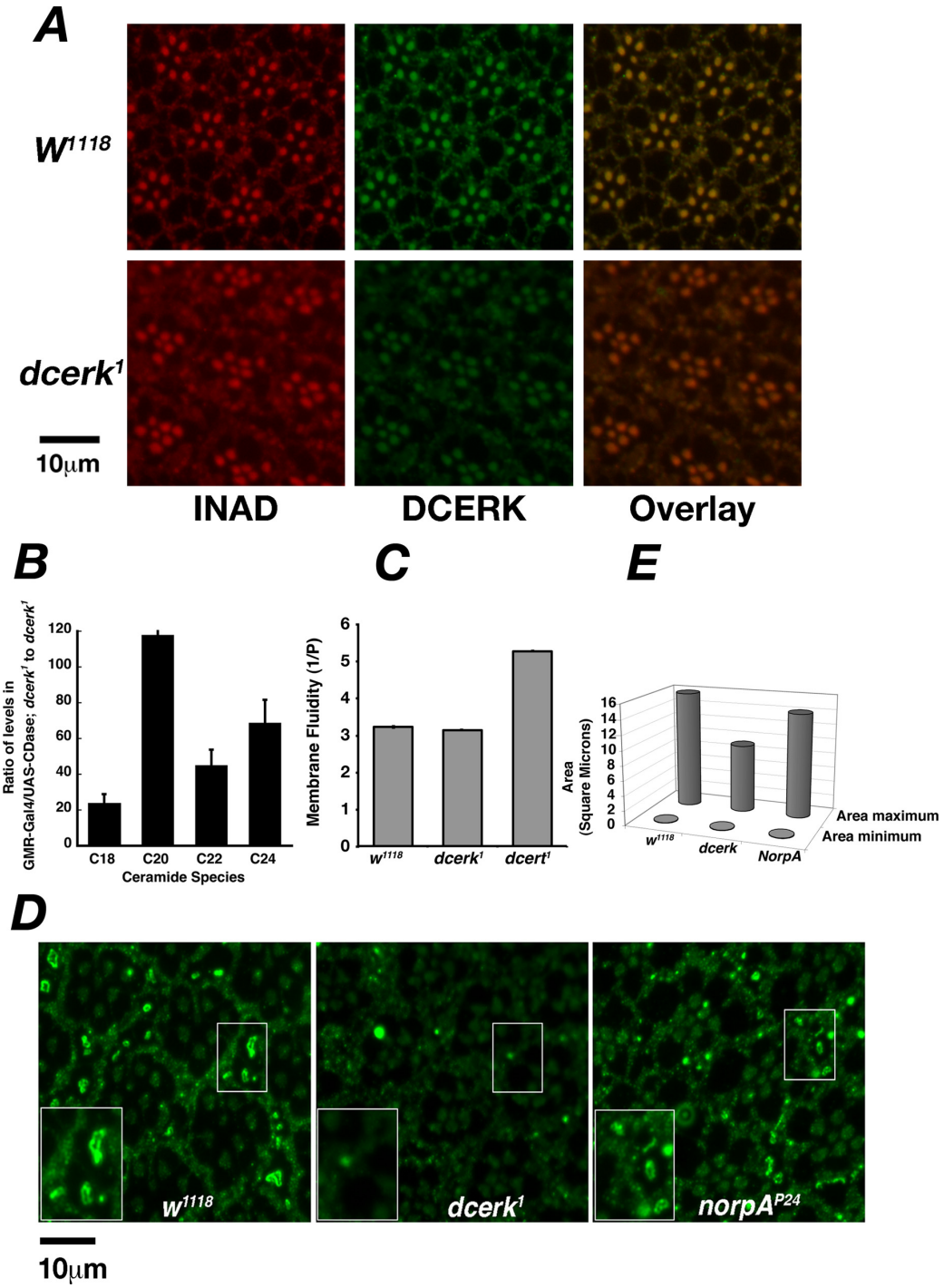

Fig. S7. CDase overexpression decreases ceramide level and rescues NORPA in *dcerk*^{1}. (*A*) Thin sections of *w*^{1118} and *dcerk*^{1} photoreceptors are immunostained for DCERK and INAD proteins. DCERK co-localizes with INAD in wild-type photoreceptors. Error bars denote standard deviation. (*B*) Ceramide levels are reduced in flies overexpressing CDase in *dcerk*^{1} mutant. Total lipids are extracted from fly heads of *dcerk*^{1} and *dcerk*^{1} overexpressing CDase and subjected to UPLC MS/MS. Individual ceramide species (with tetradecasphinganine backbone to which fatty acids of either 18, 20, 22, or 24 carbon chain are attached) are measured and values are calculated for *dcerk*^{1} overexpressing CDase relative to *dcerk*^{1}. Ceramide species with fatty acids C-18, C-22, and C-24 show decrease in ceramide compared with mutant, whereas C-20 is not rescued. (*C*) Membrane fluidity is measured in plasma membrane preparations of *w*^{1118}, *dcerk*^{1}, and *dcert*^{1} head tissue as the inverse function of fluorescence polarization. The *dcerk*^{1} does not show altered membrane fluidity compared with *w*^{1118} and *dcert*^{1}, which show an increase in membrane fluidity serves as a positive control. (*D*) Immunostaining of thin sections of *w*^{1118}, *dcerk*^{1}, and *norpA* null mutant photoreceptors with an antibody to PIP_2. Clusters of PIP_2 can be seen in *w*^{1118} and *norpA*, whereas they are less in *dcerk*^{1}. *Insets* show PIP_2 cluster in *w*^{1118}; this is not observed in *dcerk*^{1}. (*E*) Morphometric analyses of area occupied by PIP_2 clusters in *w*^{1118}, *dcerk*^{1} and *norp A* null mutant eyes. For all immunostaining experiments, nine sections from three different eyes for each condition were observed.

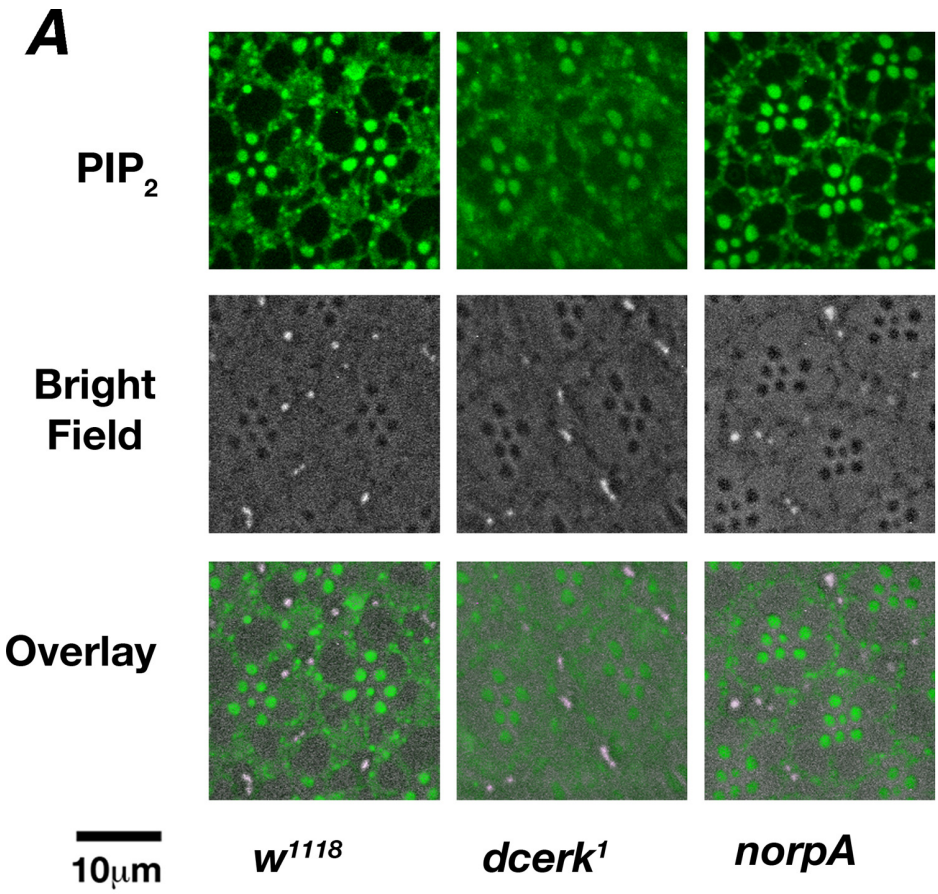

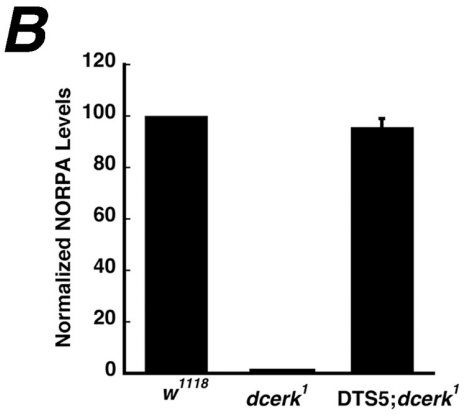

C

Diffusion Coefficient	Raft bilayer -$BrPIP_2$	Raft bilayer +$BrPIP_2$
D_{Ld} (μm²/s)	3.8±0.3	4.2±0.4
D_{Lo} (μm²/s)	0.13±0.02	0.10±0.02

Fig. S8. Immunofluorescence of thin sections of w^{1118}, $dcerk^1$, and *norpA* null photoreceptors with an antibody to PIP_2 and a quantum dot (565) conjugated secondary antibody. (*A*) Clusters of PIP_2 can be seen in w^{1118} and *norpA*, whereas they are less in $dcerk^1$. PIP_2 also appears more diffuse in $dcerk^1$ compared with w^{1118} and *norpA*. Bright field and overlay images for the three sections are also shown. (*B*) NORPA levels are comparable in $dcerk^1$ expressing *DTS5* subunit and w^{1118}. (*C*) Diffusion coefficients of the fluorescent lipid analogue BodChol in the L_d and L_o phases of SM/DOPC/cholesterol supported bilayers, without and with 3% mol $BrPIP_2$. The diffusion of the fluorescent probe is measured via line-scanning FCS and provides information about the local viscosity and the lipid packing in the membrane. Reported values (average and standard deviation) were obtained from three different positions in two independent samples.

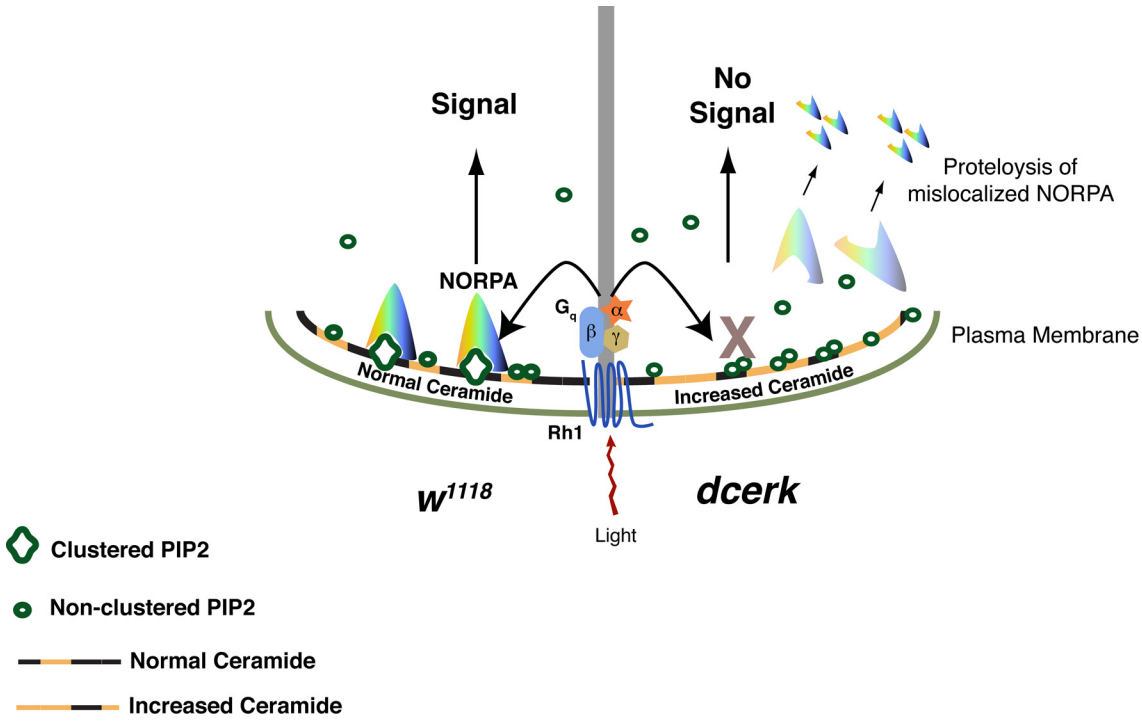

Fig. S9. Model showing ceramide kinase regulates PLC activity, function and the local organization of PIP_2 in GPCR signaling by controlling the ceramide level. In normal photoreceptors, PIP_2 that is clustered recruits NORPA to the membrane, and this leads to further downstream signaling. In *dcerk* mutant flies, the increased ceramide level perturbs the membrane microenvironment of PIP_2 correlating with degradation of NORPA. There is loss of PLC function and a failure to transduce light signal.